Airborne Cross-Source Point Clouds Fusion by Slice-to-Slice Adjustment

Shahoriar Parvaz[1], Felicia Teferle[1], Abdul Nurunnabi[1,2]

[1] Geodesy and Geospatial Engineering, Faculty of Science, Technology and Medicine, University of Luxembourg,
6, rue Richard Coudenhove-Kalergi, L-1359 Luxembourg (shahoriar.parvaz, rebecca.teferle, abdul.nurunnabi)@uni.lu
[2]Institute for Advanced Studies (IAS), University of Luxembourg, Luxembourg

Keywords: Airborne Multi-Sensor, Geospatial Data, Laser Scanning, Photogrammetry, Registration, City Modelling

Abstract

Point cloud fusion is a process plays pivotal role in geospatial data analysis that aims to integrate data from multiple sources to create a comprehensive and precise representation of the environment. Integrating point clouds acquired from cross-source or hybrid sensors presents unique challenges due to differences in geometric accuracy, precision, and the size of data gaps, along with variations in available attributes. Significant progress has been made in developing algorithms and methods to address these challenges, but the problems are not sufficiently resolved and remain one of the most challenging aspects of geospatial data processing. In this paper, we present a new approach for airborne cross-source point cloud fusion through a slice-to-slice adjustment. Our method generates cross-sectional slices and aligns them following some sequential steps. This approach enhances the accuracy and completeness of the fused point cloud, overcoming issues related to geometric disparities and data gaps. Experimental results demonstrate the effectiveness of our approach in improving registration accuracy, preserving geometric detail, and providing valuable insights for utilizing the potentials of both data sources.

1. Introduction

Light Detection and Ranging (LiDAR)-based point clouds have gained popularity for 3D data representation in various fields including computer vision, robotics, and geospatial engineering. These 3D data serve many purposes, such as object reconstruction, detection, recognition, classification and segmentation. Point clouds provide detailed and accurate representations of the environment, enabling precise analysis and understanding of the surrounding space. With the development of high-precision sensors, this technology captures millions of points of the scanned objects, provides detailed and precise information for analysis and modelling.

To capture point clouds over a large urban area, airborne laser scanning (ALS) is considered the best and most reliable technique due to its capability to provide accurate information of the scene (Mandlburger et al., 2017; Zhang et al., 2019). ALS captures detailed data for a large area quickly and efficiently. Besides, features like multiple returns make it possible to detect objects at different depths, and can capture ground objects under trees or vegetation by penetrating foliage through small gaps (Figure 1-LiDAR). This makes it a valuable tool for various applications such as forest management, city modelling, urban planning, and archaeological surveys. On the other hand, the passive sensing technology, airborne photogrammetry with subsequent dense image matching (DIM) has come into focus for urban scene 3D data collection. Also, fast-growing oblique photogrammetric sensors are being used to capture high-resolution oblique imagery from multiple angles (Figure 2), and sensors like the Leica CityMapper push it a step ahead by integrating ALS and photogrammetry (both nadir and oblique-looking) sensors on the same platform, simultaneously collecting both data types for comprehensive urban analysis (Toschi et al., 2018; Toschi, 2019). This integration allows for creating a highly detailed and more complete picture of an urban scene.

However, the problem arises when the sensors can only capture data within their limited view range, requiring them to align to generate a complete and large 3D representation, commonly known as point cloud registration (Huang et al., 2021; Li et al., 2020). This is a process of alternatively looking for correspondence and estimating the transformation matrix to minimize the geometric projection error. In addition, ALS and DIM point clouds differ significantly in terms of geometric accuracy and precision. For instance, ALS points can have a vertical accuracy of 5 cm, whereas DIM-derived points have a vertical accuracy of 10–20 cm (Zhang et al., 2019). Usually, DIM data contains more noise than ALS data, even for flat or smooth surfaces. Low-contrast images (e.g., in shadows and along narrow alleys) complicate DIM, but this is not an issue for ALS data. Due to its overhead scanning position, ALS cannot fully cover vertical elements (e.g., building facades, tree trunks, traffic signs), whereas oblique imagery can (Moe et al., 2016). Although DIM is denser than LiDAR, roof ridges are often rounded off more in the DIM than LiDAR point cloud (Mandlburger et al., 2017; Zhang et al., 2018). Additionally, the vegetation point cloud provided by DIM exhibits relative incompleteness compared to the LiDAR data. In grassy areas, this disparity leads to height differences, with the DIM point cloud registering a few centimeters higher than the corresponding LiDAR point cloud (Figure 1-DIM). Similar error matrics and geometric inconsistencies were identified between terrestrial laser scanning (TLS) and DIM point clouds (Leslar, 2015; Cavegn et al., 2014). All these above issues make the registration process challenging and require advanced algorithms and methods.

Aligning two or more point clouds in a single coherent coordinate system known as registration, whereas point cloud fusion involves combining multiple point clouds from different sources or sensors to create a single unified point cloud representing the entire scene. Fusion aims to merge information from different point clouds to create a more comprehensive and complete representation of the scanned area (Mandlburger et al., 2017). Point cloud fusion is used in various applications, including creating high-resolution 3D models, integrating data

This contribution has been peer-reviewed. The double-blind peer-review was conducted on the basis of the full paper.
https://doi.org/10.5194/isprs-annals-X-4-W4-2024-161-2024

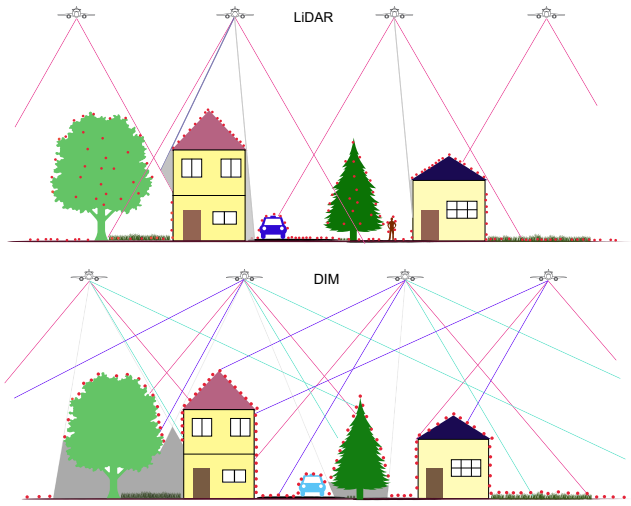

Figure 1. Data acquisition diagram using airborne LiDAR and oblique photogrammetry or DIM sensors.

from different sensors (e.g., LiDAR and photogrammetry) and improving point cloud quality. Although these two (registration and fusion) concepts may be related in some applications, they serve different purposes and are discussed in separate contexts within the literature (Abdelazeem et al., 2021; Yang et al., 2021). However, the use of different sensors to improve point cloud quality is crucial in various fields of study.

In the context of airborne LiDAR and DIM, new hybrid sensor solutions (Toschi, 2019) are rapidly entering the airborne topographic and urban mapping industry, combining both sensors on the same platform. These hybrid sensor systems provide fast and efficient large-scale point clouds and are considered essential to generating 3D models of buildings in dense urban areas. Along with this sensor, hybrid georeferencing is a recent development of traditional strip or bundle adjustment that simultaneously optimizes the relative and absolute orientation of LiDAR point clouds and aerial images (Glira et al., 2019; Haala et al., 2020). This process is particularly useful if both sensors share the same trajectory and are flown on the same platform (Toschi et al., 2018; Haala et al., 2020).

Many methods have been developed over the years for registration and fusion in relevant research fields; this paper proposes a point cloud fusion framework that utilizes line fusion techniques to integrate data from LiDAR and photogrammetric sensors. We aim to enhance the quality of the resulting point cloud by filling gaps and improving the accuracy of the DIM point cloud. Our framework leverages the complementary strengths of LiDAR and photogrammetry, such as precise distance measurements of LiDAR and detailed texture information from photogrammetry, to create a more comprehensive and accurate representation of the environment. We validate the effectiveness of our framework through extensive experiments and demonstrate its potential with real urban data by comparing the results with commonly used existing methods.

2. State-of-the-Art

Many previous studies have focused on the registration of LiDAR point clouds and aerial images separately. Few methods have explored the registration of LiDAR point clouds and aerial images together. Although optical images and ALS are georeferenced on the same coordinate system before registration, misalignment may occur due to sensor systems and systemic errors. In this section, we will discuss the existing methods and techniques for cross-source registration, as well as the challenges and potential solutions for improving the alignment accuracy between LiDAR point clouds and aerial images.

2.1 Challenges

The challenges include dealing with differences in scale, resolution, partial overlap, and geometric distortions between the LiDAR point clouds and aerial images (Huang et al., 2021; Zhang et al., 2018). These arise due to several factors, including differences in viewpoint and acquisition time, resulting in partial overlap between the captured point clouds and aerial images. This partial overlap causes discrepancies in the spatial alignment and geometric registration of multi-sensor data. One of the critical challenges in data fusion is accurately selecting correspondence points between different sensors (Tajdari et al., 2023; Chang et al., 2020). Researchers constantly explore various methods and algorithms to address this issue, but there is still no universally accepted solution. Furthermore, variations in acquisition techniques lead to discrepancies in density and noise levels within the point cloud data. Different lighting conditions, image datasets, and the dense matching algorithm (Remondino et al., 2014; Cavegn et al., 2014) can pose further challenges in accurately integrating LiDAR and DIM data. These challenges must be carefully addressed to ensure accurate alignment and merging of the two datasets. However, research shows that the fusion of LiDAR and DIM can effectively mitigate these distortions and improve the overall data quality to perform better in various applications such as urban planning, forestry management, and disaster response. It can also enhance object detection and classification accuracy.

2.2 Point Cloud Fusion

The fusion of ALS and photogrammetry-derived DIM point clouds can only be performed efficiently if they are registered precisely to eliminate the geometric inconsistency between the two different types of data (Peng et al., 2019; Toschi et al., 2021; Yang et al., 2021). This registration process entails identifying the rigid or non-rigid transformation that best aligns the points in one point cloud with the corresponding points in another point cloud (Li et al., 2021). However, most of the existing registration methods developed so far have focused on the alignment of rigid transformations. The research on non-rigid registration is still ongoing, and the development is relatively tardy compared to rigid registration (Li et al., 2021). Typically, point cloud registration methods include Iterative Closest Point (ICP) (Besl and McKay, 1992; Li et al., 2021), graph matching (Chang et al., 2020; Fu et al., 2023) and feature-based (Huang et al., 2020; Rusu et al., 2008) approaches. One feature-based deep learning method used for point cloud registration is PointNetLK (Aoki et al., 2019), which takes advantage of using the features learned by PointNet (Charles et al., 2017). Nurunnabi et al. (2021) showed that PointNet is highly sensitive to hyperparameters when dealing with large-scale ALS point clouds. However, due to its simplicity, ICP is the most used approach in practice, especially for rigid registration. Its effectiveness has limitations, such as sensitivity to outliers and tendency to fall into the local minimum. Despite its limitations, it is still widely employed as a benchmark for assessing the efficiency of new registration algorithms.

This contribution has been peer-reviewed. The double-blind peer-review was conducted on the basis of the full paper.
https://doi.org/10.5194/isprs-annals-X-4-W4-2024-161-2024 | © Author(s) 2024. CC BY 4.0 License.

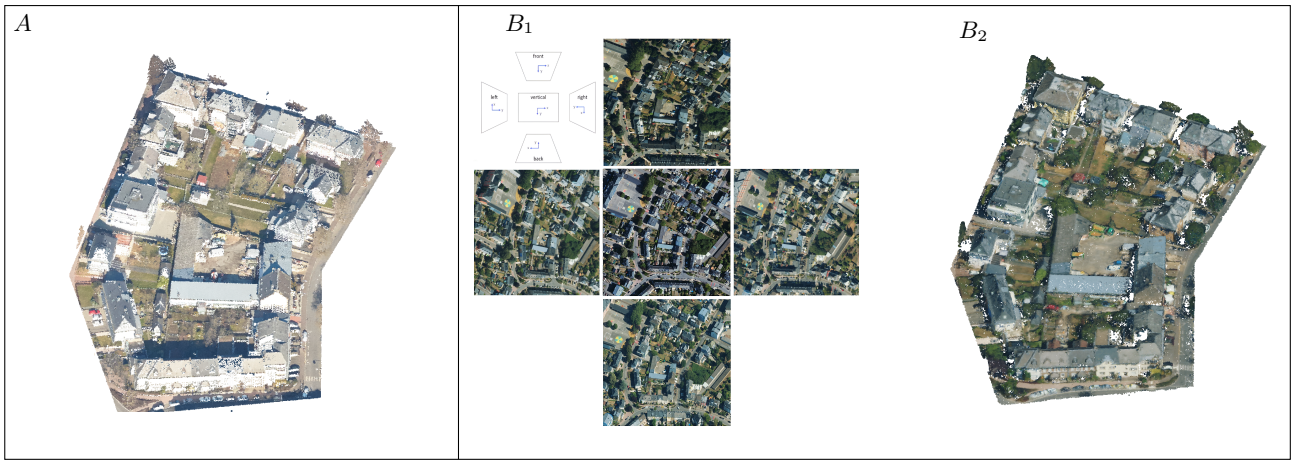

Figure 2. A sample aerial LiDAR (A), oblique imagery (B_1) and DIM points (B_2) dataset.

Most of the non-rigid registration algorithms perform better than the rigid registration algorithms when enough correspondence can be found between two point clouds Chang et al. (2020). ICP-based non-rigid registration is one of the most used methods. Like rigid registration, non-rigid registration also involves aligning multiple point clouds by iteratively establishing correspondence by nearest neighbors and updating the transformation. Although this transformation is not limited to translation and rotation, it can also include scaling, shearing, and deformation. Any non-rigid point cloud registration technique finds difficulties in aligning point clouds with large deformations or shape changes. Also, they are not robust enough to tackle noise, and outliers, and when there are gaps in the data (Ali et al., 2018). This limitation requires further research and development. In particular, developing efficient algorithms and methods that can handle these challenges is crucial. In addition, the fusion of these data is not yet reliable and efficient for feature extraction and 3D city modelling.

3. Problem Definition

Cross-source or multi-platform point cloud registration aims to align multiple point clouds acquired from different sources (LiDAR scanners, RGB-D cameras, or photogrammetry) into a common coordinate system. The main challenge of this problem lies in the fact that point clouds can have significant differences in scale, orientation, spatial distribution, and varying levels of noise and occlusion (Moe et al., 2016; Cavegn et al., 2014; Wang et al., 2023; Yu et al., 2021). These variations make it difficult to obtain satisfactory results through conventional point cloud registration methods (Wang et al., 2023). In addition, the registration process should be able to handle large-scale datasets with millions or billions of points. The goal of registration is to find a transformation matrix that maps the points from one source to the reference frame of another source, so that the overlap ratio of the two point clouds can be maximized.

Formally, given a set of N point clouds $P_1, P_2, ..., P_N$, where each point cloud P_i is defined as a set of points $P_{i,j} = (x_j, y_j, z_j)$ with $j = 1, 2, ...M$, the goal of cross-source point cloud registration is to find a set of transformation matrices $T = T_1, T_2, ..., T_N$ such that:

$$P_i' = T_j * P_i \tag{1}$$

where P_i' represents the transformed point cloud of P_i in the coordinate system of P_j. The transformation matrix T_j includes a rotation matrix R_j, a translation vector t_j, and a scaling factor s_j, such that:

$$T_j = \begin{bmatrix} R_j & t_j \\ 0 & s_j \end{bmatrix}. \tag{2}$$

The problem can be formulated as an optimization problem, where the objective function is to minimize the distance between the corresponding points of the two-point clouds (Li et al., 2020; Zhang et al., 2020). Various optimization methods, such as least-squares, maximum-likelihood estimation, and probabilistic frameworks, have been proposed. However, finding the optimal solution is often computationally expensive and requires sophisticated algorithms to handle large-scale datasets with millions or billions of points.

4. Data Preparation

4.1 LiDAR Data

Although several papers made the initial trials and demonstrated the effectiveness of airborne cross-source data, still a comprehensive open-source dataset encompassing large-scale remains unavailable (Huang et al., 2023). The preparation of LiDAR data only involves selecting the representative area from an urban scene, cropping this from larger tiles, and employing statistical outlier and noise filtering algorithms, which is essential to enhance data quality and prepare it for subsequent analyses (Nurunnabi et al., 2015). We do subsampling to avoid overlapping points and bring homogenous density over the entire point cloud, which is suggested but not required for the proposed fusion algorithm.

4.2 DIM Data

To prepare the DIM point cloud, the typical processing chain was utilized in the Agisoft Metashape software, which is based on the dense stereo matching algorithm (Remondino et al., 2014) in a multiview stereo environment. When the photogrammetric imagery does not contain georeferencing information or ground control points (GCP), a few corresponding ALS point clouds were used as GCP information within the photogrammetric bundle block adjustment (BBA). This step was carried out because the quality of combining multi-source point cloud depends on inter-dataset registration and with regards to the

LiDAR and DIM data processing chain, this registration can be categorized into four different groups (Toschi et al., 2021): (i) separate ALS stripe adjustment (SA) and bundle block adjustment (BBA), (ii) within the photogrammetric BBA use of ALS point clouds as ground control information (Yang et al., 2021), (iii) establish the transformation by using standard features (e.g., edges, boundaries, corners and 3D planar surfaces) (Peng et al., 2019), (iv) a single hybrid adjustment process with an integrated SA and BBA (Haala et al., 2020; Glira et al., 2019). Therefore, following the second category, a few corresponding ALS point clouds were used as GCP for DIM generation. Next, like LiDAR data pre-processing, we employed statistical outlier and noise-filtering algorithms also for the DIM point cloud. Finally, for the fine registration, the ICP point-to-point algorithm was employed.

5. Proposed Method

According to the definition and goal of point cloud registration and fusion, our proposed point cloud alignment algorithm meets the intent of fusion because it combines the idea of fusing two or more point clouds having different densities and distributions, collected from different sensors and perspectives into a single point cloud representation of the same scene or object. Our algorithm is primarily concerned with fusing 3D point clouds into the section view, i.e., the 2D view of a point cloud slice. Processing 3D point clouds using 2D profiles (*x*-*z*, and *y*-*z*) successfully utilized in the ground point filtering algorithm proposed by Nurunnabi et al. (2016). As far our knowledge goes, we are employing this approach, sliced-based 2D profiles, for the first time in fusion. Point cloud registration or fusion is often evaluated visually by putting a section view of both point clouds in the same window; this is the primary motivation behind the proposed algorithm. It is reasonable that if point clouds are locally fused correctly in every section, then the global accuracy of the fusion will be improved. Therefore, designing an algorithm that could accurately merge point clouds in each section of the LiDAR and DIM point clouds became imperative. As described in section 2 and Figure 3, point clouds from different sensors can vary in density, resolution, noise levels, and point gap. Due to these data variations, traditional point cloud alignment algorithms may not be suitable since they require corresponding points in both point clouds to calculate linear or non-linear transformations. Therefore, new point cloud alignment algorithms need to be developed to handle these challenges. A possible approach is to use point-to-line correspondence as a basis for transformation estimation; a representative line can be drawn in the target point cloud afterward by aligning the DIM point clouds with this line based on Euclidean distances.

Researchers have developed various algorithms and methods to fit the best line in sparse data like point clouds. Due to the complexity and distribution of urban point cloud data, polynomials usually fail to give satisfactorily fitted lines. We tried the promising and robust algorithm "LOWESS" (LOcally WEighted Scatterplot Smoothing) (Cleveland, 1979), but fails to provide the best representative line (Figure 3), which developed to approximate global function by simple local functions. Since point cloud can contain noise, and tree points cannot be represented by a line; also the main target of the proposed algorithm is to fuse planner surfaces (i.e., roof, facade, and ground), so we proposed an algorithm for applying a filtering process to sort and connect the interested points to get the best representative line of that section.

5.1 Line Drawing Algorithm

The proposed algorithm starts by applying a noise filtering method to remove unwanted points from the point cloud data. A notable robust method for noise filtering is in Nurunnabi et al. (2015). To ensure that only pertinent points are considered for line fitting, we also consider tree points as noise points based on their separation from the other points. This ensures that only relevant (linear and planar) points are considered for line fitting. First, the algorithm slices the given point cloud into small parts, processes the 2-D orthogonal projection $x-z$ or $y-z$ of the points for each slice, and sorts all the points based on their x-coordinates. Then initialize the first point as $F = (x_1, z_1)$ using the first point from the sorted array $S = (x_i, z_i)$, and assign $F = (x_1, z_1)$ in the empty array of Filtered points. The next step involves the following sequence: pick the second point from the sorted points and compute the Euclidean Distance D_i from the previous point. Repeat the same process for the next three points. Then compare the Euclidean Distance of this three-point sequence (D_j) with (D_i). If $D_i < (D_j)$, afterward, append the second point to the filtered points array and define it as the starting point for the next loop. Connect the point with the first point. Otherwise, continue to the next iteration and repeat it until the endpoint of the array S.

The output of the previous step will be an array of filtered LiDAR Point clouds $F = (x, z)$ based on their distribution and the specified distance criteria. Another output is the line, which represents the best-fit line for the LiDAR point clouds generated by connecting all the filtered points. The proposed methods for point filtering and line drawing are presented in Algorithm 1. The algorithm is applied to the *y*-*z* profile in the same way. This representative line is utilized to estimate the transformation in the fusion algorithm.

Algorithm 1: Planer points filtering and line drawing

Input:
P: LiDAR point cloud, 2D profile, $P(x, z)$
Output:
F: Filtered LiDAR Point cloud $F(x, z)$, and
a line by connected all filtered point clouds.

1. Sort the points based on their *x*-coordinates and store them in the sorted array, $S = \{(x_i, z_i)\}$.
2. Initialize the first point as $F = (x_1, z_1)$ using the first point in $S = \{(x_i, z_i)\}$.
3. Filtered points $= F$.
4. **for** $i = 2$ to size of(S) **do:**
5. $P_i = (x_i, z_i)$
6. $D_i = \sqrt{(x_i - x_{i-1})^2 + (z_i - z_{i-1})^2}$
7. $D_j = \sqrt{(x_{i+j} - x_i)^2 + (z_{i+j} - z_i)^2}$ for $j = 1, 2, 3$
8. **if** $D_i < \min(D_j)$ **then:**
9. Filtered points $=$ Filtered points $\cup (x_i, z_i)$
10. $F = P_i$
11. Connect the point with the previous point.
12. **end if**
13. Repeat Steps 5 to 11 size of S times.

5.2 Fusion Algorithm

The proposed algorithm aims to fuse DIM point cloud $Q(x, y, z)$ with LiDAR point cloud $P(x, y, z)$ to enhance the

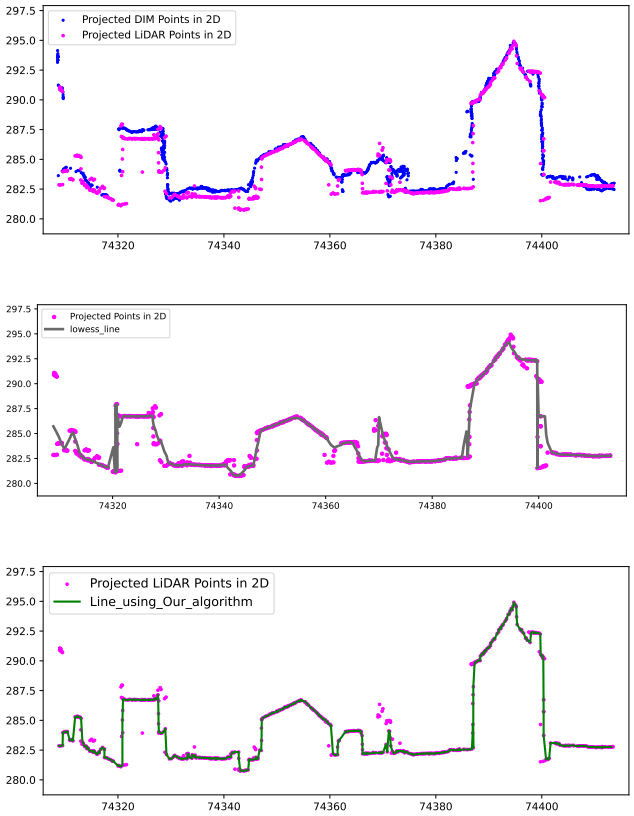

Figure 3. A strip of DIM and LiDAR points in 2D projection (Top), line drawn by LOWESS method (Middle) and our proposed method (Bottom).

accuracy and completeness of the resulting point cloud. The algorithm takes the LiDAR point cloud P, and DIM point cloud Q as inputs and fixes a threshold distance Δ used to determine the merge criterion between DIM points and the fitted line. The output is a fused point cloud, denoted as $Q_1(x_1, y_1, z_1)$.

The algorithm (Figure 4) consists of the following sequence of seven tasks:

1. **Slice generation:** For a specific y-range, both the LiDAR point cloud P and the DIM point cloud Q are sliced, creating cross-sectional planes for analysis.

2. **3D to 2D projection:** The points in each cross-sectional plane are projected onto a 2D plane defined by the x and z coordinates. This simplifies the subsequent steps.

3. **Filtering planar surface points:** The points P_i on the plane are subjected to filtering using Algorithm 1, which is designed to identify and isolate planar surface points. This filtering step helps to separate significant structural components from noise.

4. **Fitting line to planar surface:** A line is fitted to the filtered planar surface points P_i. This line serves as a reference for assessing the alignment of DIM points with the fitted line.

5. **Distance calculation:** For each DIM point Q within the same slice, the algorithm calculates the closest distance d_i between the point and the fitted line.

6. **Merging criteria check:** If the calculated distance d_i is smaller than the threshold Δ, the DIM point Q is merged with

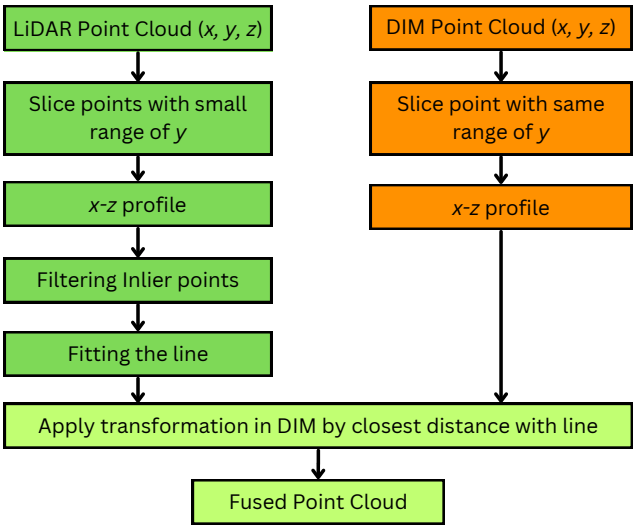

Figure 4. Fusion process for a profile in y-direction.

the fused point cloud Q_1, effectively adding it to the enhanced point cloud.

7. **Fused point cloud updating:** After evaluating all DIM points in the slice, the fused point cloud Q_1 is updated. If no DIM points satisfy the merging criteria, the original point Q remains unaltered.

The proposed airborne point cloud fusion method is illustrated in Algorithm 2. The identical approach will be used to estimate the transformation in the opposite direction on the y-z profile. We employ a combination of slicing, plane fitting, distance assessment, and merging to enhance the accuracy and completeness of the fused point cloud. By selectively integrating DIM points that align closely with the fitted line, the algorithm achieves a more accurate representation of the environment, contributing to improved point cloud analysis and applications.

Algorithm 2: Airborne point cloud fusion

Input:
P: LiDAR point cloud $P(x, y, z)$
Q: DIM Point cloud $Q(x, y, z)$
Δ: Threshold distance to merge DIM points with the fitted line
Output:
Q_1 : Fused point cloud $Q_1(x_1, y_1, z_1)$

1. For a specific y-range, make slices in both point cloud
2. Project the points in 2d plane (x,z)
3. Filtered the planner surface points P_i using Algorithm 1
4. Draw the line in the P_i
5. Find the closest distances d_i with line and points Q of same slice
6. **if** d_i smaller then Δ **then**
7. $\quad Q_1 :\leftarrow d_i + Q$
8. **end if**
9. $\quad Q_1 :\leftarrow Q$

6. Experiment and Evaluation

This section demonstrates and evaluates the proposed point cloud fusion algorithm using airborne LiDAR and DIM data-

Method		RMSE	Fitness metric	Overlap - ratio	Correspondences
ICP		0.01454	0.00042	0.00006	261
Our	1-Direction	0.01232	0.01270	0.00925	8144
	Both-Direction	0.00251	0.05511	0.07810	35195

Table 1. Comparison of algorithm accuracy for Experiment 1.

sets. Due to the superior accuracy of LiDAR sensors over airborne photogrammetry (Zhang et al., 2019; Leslar, 2015; Toschi et al., 2021), LiDAR point clouds were used as the target points and DIM as the source. This choice ensured that the fusion algorithm could achieve a high level of precision and reliability in the resulting data. In typical scenarios, airborne LiDAR and DIM exhibit accuracies of around ± 5 and $\pm 20cm$, respectively. To validate the efficacy of the fusion algorithm in this particular experiment, we employ a threshold distance value of $\Delta = 25$ cm (representing the sum of 5 cm and 20 cm) for merging DIM points with the fitted line. We evaluate the algorithm's performance visually and quantitatively using various metrics and compare it to registration algorithms.

To measure the effectiveness of the algorithm, several performance metrics were used. These include Root Mean Square Error (RMSE), fitness score, overlap ratio, and set of correspondence (Huang et al., 2017; Li et al., 2020), defined as

$$\text{RMSE} = \sqrt{\frac{\sum_{i=1}^{n} \|Q_{ci} - P_{ci}\|^2}{n}}, \tag{3}$$

$$\text{Fitness} = \frac{1}{n} \sum_{i=1}^{n} \|Q_i - P_i\|, \tag{4}$$

$$\text{Overlap Ratio} = \frac{n_{\text{overlap}}}{n_{\text{target}}}, \tag{5}$$

$$\text{Correspondence} = d(Q_i, P_j) \leq \text{max 0.02 unit distances}, \tag{6}$$

where Q_{ci} is the i-th point in the set of correspondence of source point cloud, P_{ci} is the i-th point in the set of correspondence of target point cloud, n_{overlap} is the number of overlapping points (within the threshold 0.01 unit) between source and target point clouds, n_{target} = number of points in the target point cloud, Q_i is the i-th point in the transformed source data, P_i is the i-th point in the target data. The double vertical bars $\|\cdot\|$ represent the Euclidean norm or the magnitude of the vector, and correspondence set contains pairs of indices (i, j) indicating that the i-th point in the "source" point cloud corresponds to the j-th point in the "target" point cloud if and only if $d(Q_i, P_j) \leq$max 0.02 unit distances.

6.1 Experiment 1

In the first experiment, we use airborne 3D survey mission data from the Administration of Cadastre and Topography (ACT) Luxembourg. ALS-based LiDAR, open access data, are available for the Luxembourg territory at the ACT website (https://data.public.lu/en/datasets/lidar-2019-releve-3d-du-territoire-luxembourgeois/). These data have a point density of roughly 15 points/m^2 with a horizontal precision of 3 cm and a vertical precision of 6 cm on average. The dataset is split into 500m x 500m tiles that contain between five to seven million points on average. We randomly cropped a portion from one tile scanned in Dudelange City (Figure 2). These 120m x 100m tiles have 400,921 points. On the other hand, for the airborne oblique photogrammetric or DIM points for the same area, we have used raw image data from another mission of ACT for the same territory conducted in 2020. For this mission, Leica hybrid sensors CityMapper-2 was employed, for which the camera head consists of 150 MP (14,192 x 10,640) Nadir and four oblique views (45 degrees) Leica MFC150 sensors and in a flying height of 1900m. Following the workflow explained in Section 4, we generate the input point cloud for the proposed algorithm.

Table 1 illustrates the results obtained from ICP and proposed method, which are evaluated against essential metrics. In terms of RMSE, the ICP method yielded a value of 0.01454, indicating a certain level of accuracy. However, our proposed fusion method demonstrated superior performance, achieving an RMSE of 0.01232 in the $x - z$ profile (in 1-direction) fusion variant and an even more remarkable RMSE of 0.00251 in the $x - z$ plus $y - z$ profile (considering both directions) fusion variant. Similarly, the fitness metric, which measures the closeness of points, showed favorable outcomes for the fusion method. The proposed fusion approach outperformed ICP with a fitness value of 0.01270 (1-direction) and 0.05511 (both-direction) compared to 0.00042 for the ICP method. Notably, the fusion method showcased enhanced overlap ratio results of 0.00925 (1-direction) and an impressive 0.07810 (both-direction), in contrast to the ICP result of 0.00006. Moreover, the number of correspondences found further emphasizes the fusion method's efficiency, with 8144 correspondences in the 1-direction variant and a substantial 35195 correspondences in the both-direction variant, surpassing the 261 correspondences in the ICP approach. This comprehensive comparison underscores the robustness and accuracy of the proposed fusion method in addressing the challenges posed by the dataset. Also, the results (Figure 5) demonstrate the effectiveness of our approach in improving data accuracy and preserving geometric details

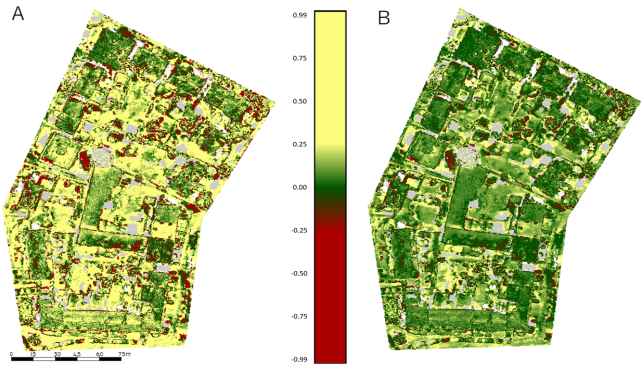

Figure 5. Colour-coded height differences between LiDAR and DIM, (A) before fusion, and (B) after fusion. (Experiment 1)

6.2 Experiment 2

In the second experiment, we use another set of ALS and photogrammetry data collected over Dublin City in 2015 (Laefer et al., 2017). ALS was carried out by using a TopEye system S/N 443. Imagery data was captured using a Phase One camera system. The average flying altitude was 300m. We cropped a representative part of the data, which covers 250m x 250m areas. Following the process described in Section 4, we prepare the LiDAR and DIM point clouds for the final fusion. After applying the fusion algorithm, the results show that the

Method		RMSE	Fitness metric	Overlap - ratio	Correspondences
ICP		0.01550	0.00144	0.00022	7480
Our	1-Direction	0.01153	0.07608	0.05773	506221
	Both-Direction	0.00383	0.22927	0.33079	1537927

Table 2. Comparison of algorithm accuracy for Experiment 2.

proposed method is highly successful for airborne multi-sensor point cloud fusion (Figure 6). For quantitative evaluation of the proposed algorithm, we calculate all the above-mentioned matrices. Table 2 presents all the results from this experiment. Although Dublin city data sets are aligned more than ACT data, the proposed fusion algorithm still shows its effectiveness in increasing accuracy in every metrics.

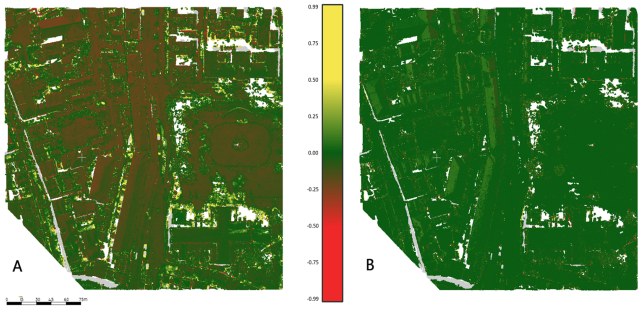

Figure 6. Colour-coded height differences between LiDAR and DIM, (A) before fusion, and (B) after fusion. (Experiment 2)

One of the major challenges in cross-source point cloud fusion is setting up the correspondence points between different point clouds. After deploying our method, we successfully established more correspondence points than the established method, which indicates achieving a more accurate alignment of urban cross-source point clouds. These metrics gave us a full picture of how well an algorithm worked, and we found that our algorithm consistently outperformed the existing ICP method in terms of accuracy and alignment of urban cross-source point clouds. Moreover, this clarification is evident in the color-coded height differences between LiDAR and DIM (Figures 5 and 6). The results show the effectiveness and accuracy of the algorithm in producing a complete set of dense data for potential use in various applications.

7. Conclusion

This paper presented a study on cross-source urban point cloud fusion, addressing the challenges of integrating diverse point cloud data from various sources. We demonstrated the effectiveness of the proposed fusion method in improving the precision, completeness, and diversity of urban point clouds through a systematic analysis. The fusion approach presented in the paper tried to mitigate the limitations of individual point cloud datasets and enabled the seamless integration of multiple sources, resulting in a more complete representation of urban environments. The results showed a significant improvement in the merged point cloud data quality.

The methodology was validated through two experiments and comparison studies against existing technique. The results showcased the superior performance of the proposed fusion technique in handling data from diverse sources, yielding highly accurate and detailed representations of complex urban structures. This paper focuses principally on airborne LiDAR and DIM data to demonstrate the effectiveness of the fusion method in enhancing the accuracy and detail of complex urban structures. Depending on two user-defined parameters: slice thickness and fusion threshold distance, the approach can be customized to meet specific project requirements. For future research, it would be beneficial to investigate the potential impact of different user-defined parameters on the accuracy and efficiency of the method. We also recommend exploring the approach's applicability in various domains. Further research will be conducted to make the method more automatic by using adaptive parameter localization.

Acknowledgements

This study is funded through Project No 17042266, DF4CM - Reporting/22/IS, Luxembourg National Research Fund (FNR). We also thank the Administration du Cadastre et de la topographie (ACT) for the Airborne oblique imagery and LiDAR dataset. Abdul Nurunnabi is funded through the IAS-AUDACITY-PIONEER-2022 project at the University of Luxembourg.

References

Abdelazeem, M., Elamin, A., Afifi, A., El-Rabbany, A., 2021. Multi-sensor point cloud data fusion for precise 3D mapping. *The Egyptian Journal of Remote Sensing and Space Science*, 24(3, Part 2), 835 – 844.

Ali, S. A., Golyanik, V., Stricker, D., 2018. Nrga: Gravitational approach for non-rigid point set registration. *International Conference on 3D Vision (3DV)*, 756 – 765.

Aoki, Y., Goforth, H., Srivatsan, R. A., Lucey, S., 2019. Pointnetlk: Robust efficient point cloud registration using pointnet. *IEEE Conference on Computer Vision and Pattern Recognition (CVPR)*, 7156 – 7165.

Besl, P., McKay, N. D., 1992. A method for registration of 3-D shapes. *IEEE Transactions on Pattern Analysis and Machine Intelligence*, 14(2), 239 – 256.

Cavegn, S., Haala, N., Nebiker, S., Rothermel, M., Tutzauer, P., 2014. Benchmarking high density image matching for oblique airborne imagery. *The International Archives of the Photogrammetry, Remote Sensing and Spatial Information Sciences*, XL-3, 45 – 52.

Chang, S., Ahn, C., Lee, M., Oh, S., 2020. Graph-matching-based correspondence search for nonrigid point cloud registration. *Computer Vision and Image Understanding*, 192, 102899.

Charles, R. Q., Su, H., Kaichun, M., Guibas, L. J., 2017. Pointnet: Deep learning on point sets for 3d classification and segmentation. *IEEE Conference on Computer Vision and Pattern Recognition (CVPR)*, 77 – 85.

Cleveland, W. S., 1979. Robust locally weighted regression and smoothing scatterplots. *Journal of the American Statistical Association*, 74(368), 829 – 836.

Fu, K., Luo, J., Luo, X., Liu, S., Zhang, C., Wang, M., 2023. Robust point cloud registration framework based on deep graph matching. *IEEE Transactions on Pattern Analysis and Machine Intelligence*, 45(5), 6183 – 6195.

Glira, P., Pfeifer, N., Mandlburger, G., 2019. Hybrid orientation of airborne LiDAR point cloud and aerial images. *ISPRS Annals of the Photogrammetry, Remote Sensing and Spatial Information Sciences*, IV-2/W5, 567 – 574.

Haala, N., Kölle, M., Cramer, M., Laupheimer, D., Mandlburger, G., Glira, P., 2020. Hybrid georeferencing, enhancement and classification of ultra-high resolution UAV LiDAR and image point cloud for monitoring applications. *ISPRS Annals of the Photogrammetry, Remote Sensing and Spatial Information Sciences*, V-2-2020, 727 – 734.

Huang, X., Mei, G., Zhang, J., 2020. Feature-metric registration: A fast semi-supervised approach for robust point cloud registration without correspondences. *IEEE Conference on Computer Vision and Pattern Recognition (CVPR)*, 11363 – 11371.

Huang, X., Mei, G., Zhang, J., 2023. Cross-source point cloud registration: Challenges, progress and prospects. *Neurocomputing*, 548, 126383.

Huang, X., Mei, G., Zhang, J., Abbas, R., 2021. A comprehensive survey on point cloud registration.

Huang, X., Zhang, J., Fan, L., Wu, Q., Yuan, C., 2017. A systematic approach for cross-Source point cloud registration by preserving macro and micro structures. *IEEE Transactions on Image Processing*, 26(7), 3261 – 3276.

Laefer, D., Abuwarda, S., Vo, A.-V., Truong-Hong, L., Gharibi, H., 2017. 2015 aerial laser and photogrammetry survey of dublin city collection record.

Leslar, M., 2015. Integrating terrestrial LiDAR with point created from unmanned aerial vehicle imagery. *The International Archives of the Photogrammetry, Remote Sensing and Spatial Information Sciences*, XL-1/W4, 97 – 101.

Li, L., Wang, R., Zhang, X., 2021. A tutorial review on point cloud registrations: principle, classification, comparison, and technology challenges. *Mathematical Problems in Engineering*.

Li, P., Wang, R., Wang, Y., Tao, W., 2020. Evaluation of the ICP algorithm in 3D point cloud registration. *IEEE Access*, 8, 68030 – 68048.

Mandlburger, G., Wenzel, K., Spitzer, A., Haala, N., Glira, P., Pfeifer, N., 2017. Improved topographic models via concurrent airborne LiDAR and dense image matching. *ISPRS Annals of the Photogrammetry, Remote Sensing and Spatial Information Sciences*, IV-2/W4, 259 – 266.

Moe, K., Toschi, I., Poli, D., Lago, F., Schreiner, C., Legat, K., Remondino, F., 2016. Changing the production pipeline - use of oblique aerial cameras for mapping purposes. *The International Archives of the Photogrammetry, Remote Sensing and Spatial Information Sciences*, XLI-B4, 631 – 637.

Nurunnabi, A., Teferle, F. N., Li, J., Lindenbergh, R. C., Parvaz, S., 2021. Investigation of PointNet for semantic segmentation of large-scale outdoor point clouds. *The International Archives of the Photogrammetry, Remote Sensing and Spatial Information Sciences*, XLVI-4/W5-2021, 397 – 404.

Nurunnabi, A., West, G., Belton, D., 2015. Outlier detection and robust normal-curvature estimation in mobile laser scanning 3D point cloud data. *Pattern Recognition*, 48(4), 1404 – 1419.

Nurunnabi, A., West, G., Belton, D., 2016. Robust locally weighted regression techniques for ground surface points filtering in mobile laser scanning three dimensional point cloud data. *IEEE Transactions on Geoscience and Remote Sensing*, 54(4), 2181 – 2193.

Peng, S., Ma, H., Zhang, L., 2019. Automatic registration of optical images with airborne LiDAR point cloud in urban scenes based on line-point similarity invariant and extended collinearity equations. *Sensors*, 19(5).

Remondino, F., Spera, M. G., Nocerino, E., Menna, F., Nex, F., 2014. State of the art in high density image matching. *The Photogrammetric Record*, 29(146), 144 – 166.

Rusu, R. B., Blodow, N., Marton, Z. C., Beetz, M., 2008. Aligning point cloud views using persistent feature histograms. *IEEE international conference on intelligent robots and systems*, IEEE, 3384 – 3391.

Tajdari, F., Huysmans, T., Song, Y., 2023. Non-rigid registration via intelligent adaptive feedback control. *IEEE Transactions on Visualization and Computer Graphics*, 1 – 17.

Toschi, I., 2019. Airborne oblique imaging: towards the hybrid era. *Archives of Photogrammetry, Cartography and Remote Sensing*, 31(1), 21 – 28.

Toschi, I., Farella, E., Welponer, M., Remondino, F., 2021. Quality-based registration refinement of airborne LiDAR and photogrammetric point clouds. *ISPRS Journal of Photogrammetry and Remote Sensing*, 172, 160 – 170.

Toschi, I., Remondino, F., Rothe, R., Klimek, K., 2018. Combining airborne oblique camera and LiDAR sensors: investigation and new perspectives. *The International Archives of the Photogrammetry, Remote Sensing and Spatial Information Sciences*, XLII-1, 437 – 444.

Wang, Y., Bu, S., Chen, L., Dong, Y., Li, K., Cao, X., Li, K., 2023. Hybridfusion: Lidar and vision cross-source point cloud fusion.

Yang, W., Liu, Y., He, H., Lin, H., Qiu, G., Guo, L., 2021. Airborne LiDAR and photogrammetric point cloud fusion for extraction of urban tree metrics according to street network segmentation. *IEEE Access*, 9, 97834 – 97842.

Yu, H., Li, F., Saleh, M., Busam, B., Ilic, S., 2021. CoFiNet: Reliable Coarse-to-fine Correspondences for Robust PointCloud Registration. *Advances in Neural Information Processing Systems*, 34.

Zhang, Z., Dai, Y., Sun, J., 2020. Deep learning based point cloud registration: an overview. *Virtual Reality and Intelligent Hardware*, 2(3), 222 – 246.

Zhang, Z., Gerke, M., Vosselman, G., Yang, M. Y., 2018. A patch-based method for the evaluation of dense image matching quality. *International Journal of Applied Earth Observation and Geoinformation*, 70, 25 – 34.

Zhang, Z., Vosselman, G., Gerke, M., Persello, C., Tuia, D., Yang, M. Y., 2019. Detecting building changes between airborne laser scanning and photogrammetric data. *Remote Sensing*, 11(20).